Cyclometalation Reactions on Rhodium(I). Evidence for a Chelate Effect and Competing C−H and C−O Oxidative Additions

Sven Sjövall, Carlaxel Andersson, and Ola F. Wendt*

Inorganic Chemistry, Department of Chemistry, Lund University, P.O. Box 124, S-221 00 Lund, Sweden

Received June 21, 2001

The ligand $Ph_2PC_6H_4(CH_2N(Me)CO(Et))$ reacts with (bis(diphenylphosphino)butane)(2,5-norbornadiene)rhodium tetrafluoroborate (**2a**) and (bis(diphenylphosphino)ethane)(2,5-norbornadiene) rhodium tetrafluoroborate (**2b**) at room temperature in the presence of hydrogen to displace the norbornadiene and give the chelate complexes **3a**,**b**, in which the phosphorus and the oxygen atoms are coordinated to give an eight-membered ring. At elevated temperatures these complexes are converted into cyclometalated Rh(III) benzyl hydride complexes. Rate law, activation parameters, and reactivity trends of this latter transformation indicate that displacement of one of the phosphine functionalities of the bis-chelating phosphine takes place before the C−H activation. Complex **3b** was characterized by X-ray crystallography. On the other hand, under ambient conditions the ligand (±)-$Ph_2PC_6H_4(CH(Me)O(CO)Et)$ undergoes activation of either the benzylic C−O or C−H bond, depending on the nature of the Rh precursor used. Thus, **2b** gives overall elimination of propionic acid to result in a styrene complex, which was characterized by X-ray crystallography, whereas bis(2,5-norbornadiene)rhodium tetrafluoroborate gives a mixture of Rh(III) benzyl hydride stereoisomers. The difference in reactivity is discussed in terms of different mechanisms for the two processes.

Introduction

Homogeneous C−X (X = H, C) bond activation by transition-metal complexes is a field of much current interest, with the overall objective of designing new selective and efficient processes for the utilization of hydrocarbons.[1] Not only has the normally more favorable C−H bond activation process been extensively studied[2] but also important synthetic and mechanistic insights into the C−C bond activation process have been realized recently.[3,4] It has been shown by numerous examples that the competing reactions of either C−H or C−C bond activation can be controlled by a careful choice of either the substrate or the metal complex, e.g. by the use of strained alkanes,[4a−c] prearomatic systems,[4d,e] agostic interactions,[4f,g] clusters,[4h,i] and sterically demanding systems.[4j,k] Due to their relatively convenient preparations, the majority of the complexes studied are of the cyclometalated type, especially those that are ortho-metalated. Such complexes are characterized by their high thermal stability due to the energetically strong M−X bond and the chelate ring formed upon the intramolecular chelate-assisted C−X bond activation. Because of these beneficial features, as a "side effect", the use of metallacyclic complexes in catalysis has grown into a major field of its own.[5]

Two of us have recently demonstrated that the triphenylphosphine derivatives *N*-methyl-*N*-propionyl-2-(diphenylphosphino)benzylamine (DPPAM; **1a**) and 1-(2-diphenylphosphino)benzyl propionate (**1b**) (Chart 1) undergo facile insertion of a Rh(I) or Ir(I) metal center into one of its benzylic C−H bonds.[6] These tridentately PCO-coordinated phosphines are an important class of ligands, since they produce a rather unusual complex with a hydride and a σ-alkyl group in its coordination

* To whom correspondence should be addressed. E-mail: ola.wendt@inorg.lu.se.

(1) (a) Crabtree, R. H. *Angew. Chem., Int. Ed. Engl.* **1993**, *32*, 789. (b) Crabtree, R. H. *Chem. Rev.* **1985**, *85*, 245.

(2) For excellent reviews see: (a) Arndtsen, B. A.; Bergman, R. G.; Mobley, T. A.; Peterson, T. H. *Acc. Chem. Res.* **1995**, *28*, 154. (b) Canty, A. J.; van Koten, G. *Acc. Chem. Res.* **1995**, *28*, 406. (c) Schneider, J. J. *Angew. Chem., Int. Ed. Engl.* **1996**, *35*, 1068. (d) Ryabov, A. D. *Chem. Rev.* **1990**, *90*, 403. (e) Stahl, S.; Labinger, J. A.; Bercaw, J. E. *Angew. Chem., Int. Ed. Engl.* **1998**, *37*, 2181.

(3) Rybtchinski, B.; Milstein, D. *Angew. Chem., Int. Ed.* **1999**, *38*, 870.

(4) (a) Cassar, L.; Halpern, J. *J. Chem. Soc. D* **1970**, 1082. (b) Cassar, L.; Eaton, P. E.; Halpern, J. *J. Am. Chem. Soc.* **1970**, *92*, 3515. (c) Periana, R. A.; Bergman, R. G. *J. Am. Chem. Soc.* **1986**, *108*, 7346. (d) Eilbracht, P. *Chem. Ber.* **1980**, *113*, 542. (e) Urbanos, F.; Halcrow, M. A.; Fernandez-Baeza, J.; Dahan, F.; Labroue, D.; Chaudret, B. *J. Am. Chem. Soc.* **1993**, *115*, 3484. (f) Bennett, M. A.; Nicholls, J. C.; Rahman, A. K. F.; Redhouse, A. D.; Spencer, J. L.; Willis, A. C. *J. Chem. Soc., Chem. Commun.* **1989**, 1328. (g) Nicholls, J. C.; Spencer, J. L. *Organometallics* **1994**, *13*, 1781. (h) Ingman, S. L.; Johnson, B. F. G.; Martin, C. M.; Parker, D. G. *J. Chem. Soc., Chem. Commun.* **1995**, 159. (i) Brown, D. B.; Dyson, P. J.; Johnson, B. F. G.; Martin, C. M.; Parker, D. G.; Parsons, S. *J. Chem. Soc., Dalton Trans.* **1997**, 1909. (j) Rybtchinski, B.; Vigalok, A.; Yehoshoa, B.-D.; Milstein, D. *J. Am. Chem. Soc.* **1996**, *118*, 12406. (k) Gandelman, M.; Vigalok, A.; Shimon, L. J. W.; Milstein, D. *Organometallics* **1997**, *16*, 3981.

(5) For important examples see: (a) Lewis, L. *J. Am. Chem. Soc.* **1986**, *108*, 743. (b) Bergbreiter, D. E.; Osburn, P. L.; Liu, Y.-S. *J. Am. Chem. Soc.* **1999**, *121*, 9531. (c) Donkervoort, J. G.; Vicario, G. L.; Jastrzebski, J. T. B. H.; Gossage, R. A.; Cahiez, G.; van Koten, G. *J. Organomet. Chem.* **1998**, *558*, 61. (d) Beletskaya, I. P.; Cheprakov, A. V. *Chem. Rev.* **2000**, *100*, 3009. (e) Steenwinkel, P.; Gossage, R. A.; van Koten, G. *Chem. Eur. J.* **1998**, *4*, 759.

(6) (a) Sjövall, S.; Kloo, L.; Nikitidis, A.; Andersson, C. *Organometallics* **1998**, *17*, 579. (b) Sjövall, S.; Johansson, M.; Andersson, C. *Organometallics* **1999**, *18*, 2198. (c) Sjövall, S.; Svensson, P. H.; Andersson, C. *Organometallics* **1999**, *18*, 8, 5412.

10.1021/om010543x CCC: $20.00
Publication on Web 10/10/2001

Chart 1

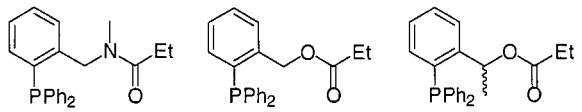

sphere.[7] Here we report a mechanistic study regarding the C−H activation process of our PCO system based on kinetics and structure−reactivity arguments. Moreover, an unusual example of competition between C−H and C−O activation on a tertiary carbon center is presented.

Results and Discussion

Ligands. Hemilabile phosphines are advantageous ligands for the study of oxidative processes, especially cyclometalation, since upon coordination to a transition-metal center the pendant side chain promotes chelate-assisted intramolecular oxidative insertion of the metal center. The PCO ligands previously reported by us (Chart 1) are good examples, and with these species cyclometalation is exceptionally facile, due to the resulting formation of a bis-chelating five-membered-ring structure.[6] To further investigate the C−H bond activation process with the PCO system, including a possible competition between oxidative addition of C−H and C−C bonds, we have synthesized the functionalized phosphine (±)-DPPES ((±)-1-(2-(diphenylphosphino)-phenyl)ethyl propionate; **1c**) (Chart 1). The new phosphine **1c** was obtained by reducing 1-(2-(diphenylphosphino)phenyl)ethanone to give (±)-1-(2-(diphenylphosphino)phenyl)ethanol, which was then reacted with propionyl chloride in THF (Scheme 1). Characteristic

Scheme 1

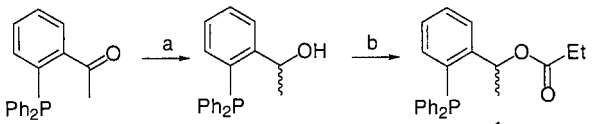

spectroscopic features for the racemic mixture of **1c** are the singlet exhibited at −17.3 ppm ($^{31}P\{^1H\}$ NMR), the strong vibrational absorption for the carbonyl group at 1729 cm^{-1} (IR), and the doublet displayed at 70.0 ppm ($^3J_{PC}$ = 28.1 Hz) for the tertiary benzylic carbon ($^{13}C\{^1H\}$ NMR).

Complexation of DPPAM (1a) with Bis-Phosphine Rhodium Precursors. A dichloromethane solution of the rhodium bis-phosphine complex [Rh(DPPB)(NBD)][BF_4] (**2a**; DPPB = bis(1,2-diphenylphosphino)-butane, NBD = 2,5-norbornadiene) and 1 equiv of ligand **1a**, stirred for 40 min under an atmosphere of molecular hydrogen at room temperature, yields after workup the four-coordinate Rh(I) complex **3a** (Scheme 2). This complex was unambiguously characterized by NMR and IR spectroscopy. The $^{31}P\{^1H\}$ NMR spectrum of **3a** displays three doublets of doublets of doublets posi-

Scheme 2

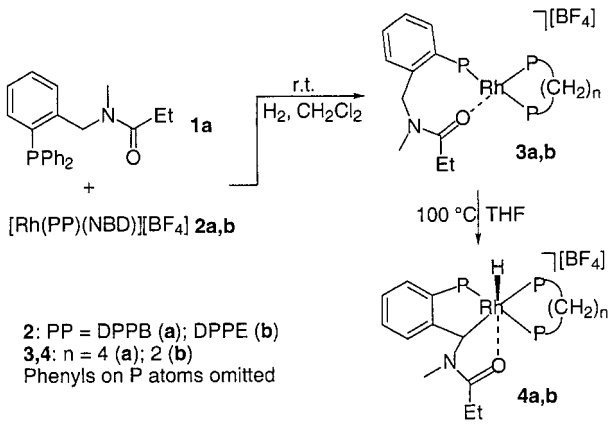

tioned at 48.9 ($^1J_{RhP}$ = 188.5 Hz, $^2J_{PP}$ = 51.1, 34.5 Hz, P_{DPPB}), 39.0 ($^1J_{RhP}$ = 145.1 Hz, $^2J_{PP}$ = 302.7, 51.1 Hz, P_{DPPB}) and 30.3 ppm ($^1J_{RhP}$ = 132.3 Hz, $^2J_{PP}$ = 302.7, 34.5 Hz, P_{DPPAM}). The lack of a symmetry plane in complex **3a** results in diastereotopic protons in the benzylic group, and these are displayed in the ^1H NMR spectrum as broad doublets at 8.98 ($^2J_{HH}$ = 14.4 Hz) and 3.81 ppm ($^2J_{HH}$ = 14.4 Hz), respectively. The far downfield shift for one of them indicates a significant through-space interaction with the metal center. In addition, the $^{13}C\{^1H\}$ NMR spectrum of **3a** displays a singlet for the benzylic carbon in the normal aliphatic region (29.5 ppm). The carbonyl stretching frequency, positioned at 1586 cm^{-1}, is shifted to a lower wavenumber compared to the free ligand (1655 cm^{-1}),[8] verifying the eight-membered-ring structure in the complex resulting from coordination of the carbonyl group to the rhodium atom.

The inability of **3a** to cyclometalate at room temperature was unexpected, since the analogous mono-phosphine precursor complex [Rh(PPh_3)$_2$(NBD)][PF_6] readily yields a bis-chelating PCO complex with DPPAM when using the same reaction conditions as for the synthesis of **3a**.[6c] Clearly, the DPPB ligand in **3a** is not innocent but influences the course of the reaction. To further investigate the possible steric effects, the reaction was repeated, but now with [Rh(DPPE)[NBD)][BF_4] (**2b**) (DPPE = bis(1,2-diphenylphosphino)ethane) as the diphosphine precursor (Scheme 2), bearing in mind the differences in bite angles for DPPE (78°) and DPPB (98°).[9] The structure of **3b** is identical with that for **3a**, as determined by multinuclear NMR spectroscopy. The $^{31}P\{^1H\}$ NMR spectrum of **3b** exhibits three doublets of doublets of doublets at 79.4 ($^1J_{RhP}$ = 195.9 Hz, $^2J_{PP}$ = 37.3, 30.9 Hz, P_{DPPE}), 66.3 ($^1J_{RhP}$ = 144.7 Hz, $^2J_{PP}$ = 308.9, 37.3 Hz, P_{DPPE}), and 29.4 ppm ($^1J_{RhP}$ = 127.3 Hz, $^2J_{PP}$ = 308.9, 30.9 Hz, P_{DPPAM}). The signals for the diastereotopic benzylic protons appear in the ^1H NMR spectrum at 8.48 ($^2J_{HH}$ = 13.6 Hz) and 4.07 ppm ($^2J_{HH}$ = 13.6 Hz) while the benzylic carbon appears at 35.7 ppm in the $^{13}C\{^1H\}$ NMR spectrum; the assignments were verified by an HMQC NMR experiment. The molecular structure of **3b** was confirmed by X-ray crystallography, which also revealed an agostic interac-

(7) (a) Zhang, L.; Zetterberg, K. *Organometallics* **1991**, *10*, 3806. (b) Rybtchinski, B.; Konstantinovsky, L.; Shimon, L. J. W.; Vigalok, A.; Milstein, D. *Chem. Eur. J.* **2000**, *6*, 3287.

(8) Nikitidis, A.; Andersson, C. *Phosphorus, Sulfur Silicon Relat. Elem.* **1993**, *78*, 141.

(9) del Rio, I.; Ruiz, N.; Claver, C.; van der Veen, L. A.; van Leuween, P. W. N. M. *J. Mol. Catal. A* **2000**, *161*, 39.

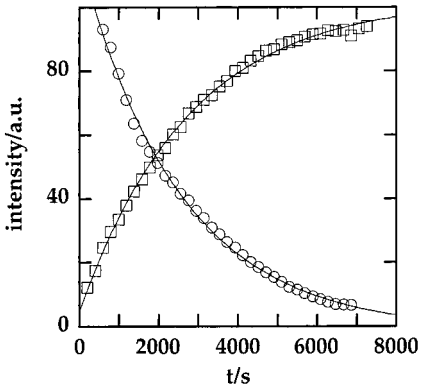

Figure 1. ^{1}H NMR peak intensities of the N−CH_3 protons for complex **3b** (○) and **4b** (□) in 1,1,2,2-tetrachloroethane-d_2 as a function of time. The solid lines denote the best fit to single exponentials. T = 352.7 K.

tion for the benzylic proton appearing in the downfield region in the ^{1}H NMR spectrum (vide infra).

The difficulty for DPPAM to cyclometalate at room temperature, no matter the steric property of the rhodium bis-phosphine precursor used, could imply that dissociation of one phosphine functionality to form an unsaturated three-coordinate Rh(I) species takes place before or during the rate-determining step in the cyclometalation. To induce C−H activation, complexes **3a**,**b**, separately dissolved in 1,1,2,2-tetrachloroethane-d_2, were heated to 70 °C in closed NMR tubes. Both samples were monitored by ^{1}H NMR spectroscopy, which revealed formation of C−H activation products within minutes, e.g. by the appearance of hydride signals at −17.2 (**4a**) and −17.4 ppm (**4b**), and after 3 h both conversions were complete. Complexes **4a**,**b** were synthesized on a preparatory scale by heating THF solutions of **3a**,**b** at 100 °C in closed vessels for 90 min (Scheme 2). The complexes were characterized by NMR and IR spectroscopy. The tridentate PCO coordination of the DPPAM ligand is manifested by the strong downfield shifts in their ^{31}P{^{1}H} NMR spectra (56.1 (**4a**) and 61.9 ppm (**4b**)), the carbonyl stretching frequencies in the IR spectra (1571 cm^{-1} (**4a**) and 1572 cm^{-1} (**4b**)), and the benzylic carbon signals in their ^{13}C{^{1}H} NMR spectra (multiplets at 72.6 (**4a**) and 70.9 ppm (**4b**)).

Kinetics of Formation of 4b. Qualitative experiments showed that **3a**,**b** undergo cyclometalation at approximately the same rate. The kinetics of the conversion of **3b** was more well-behaved, and this complex was chosen for a more careful analysis. The reaction was monitored at temperatures ranging from 332.7 to 362.7 K in 1,1,2,2-tetrachloroethane-d_2 using ^{1}H NMR spectroscopy. The intensities of the NCH_3 singlets for both **3b** and **4b** were followed as a function of time, and the data so obtained was fitted to single exponentials. A typical fit (at 352.7 K) is shown in Figure 1, giving rate constants of $(4.0 \pm 0.3) \times 10^{-4}$ and $(3.6 \pm 0.2) \times 10^{-4}$ s^{-1} for the consumption of reactant and formation of product, respectively. Only **3b** and **4b** were observed during the reaction, and the conversion is thus a single process which is first order in rhodium complex. Average rate constants at each temperature were computed, and the data were fitted to the Eyring equation as shown in Figure 2. Activation parameters are $\Delta H^{\ddagger} = 78 \pm 6$ kJ mol^{-1} and $\Delta S^{\ddagger} = -90 \pm 16$ J K^{-1} mol^{-1}.

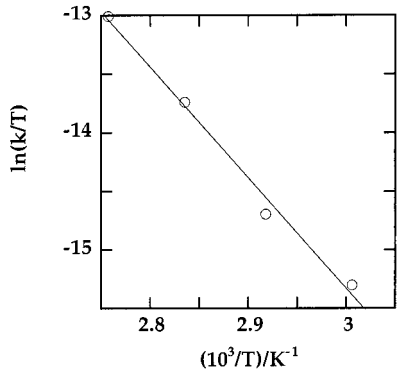

Figure 2. Eyring plot for the conversion of **3b** to **4b**. First-order rate constants are 0.75×10^{-4}, 1.42×10^{-4}, 3.80×10^{-4}, and 8.14×10^{-4} s^{-1} at 332.7, 342.7, 352.7, and 362.7 K, respectively.

Mechanism of C−H Activation. The reactivity patterns, where the complexes with chelating phosphines display a much lower reactivity as compared to the triphenylphosphine complex, indicates that the phosphines are not only innocent spectator ligands. Secondary effects, e.g. steric hindrance, can probably also be ruled out, since DPPE and DPPB would be expected to behave differently in this respect as opposed to what is observed. Chelating phosphines are generally more difficult to displace/ring-open, and this is the most likely explanation for the lower reactivity of the chelate complexes. Thus, phosphine displacement/opening of the chelate ring most probably takes place prior to or during the rate-determining step of the C−H activation. This is in agreement with the rate law, but its simple form of course makes it compatible with a large number of mechanisms. Unfortunately, it was not possible to check the effect of adding free phosphine, since this causes extrusion of the P,O chelate. The activation parameters clearly speak against simple dissociation as the rate-determining step; the entropy is negative and the enthalpy is too low to correspond to a Rh−P bond dissociation energy. We therefore favor an explanation in which reaction takes place via an intermediate from which then the actual oxidative addition occurs irreversibly (Scheme 3). The observed activation parameters are then a sum of those relating to the individual rate constants in the reaction scheme. The structure of the intermediate is to some extent speculative. One possibility is shown in Scheme 3, in which the P,O ligand is coordinated in a trans fashion with one of the arms of the DPPE being pendant. This opens up a possibility for the C−H bond to coordinate in a η^2 fashion, thus producing two five-membered rings. Such a well-ordered intermediate where the orbitals are arranged to facilitate the electron transfer would give a negative contribution to the observed entropy of activation, explaining its negative value. The formation

Scheme 3

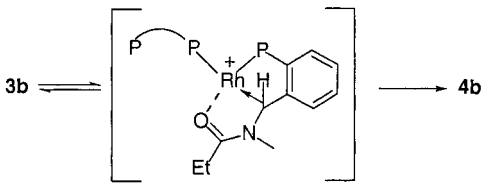

Scheme 4

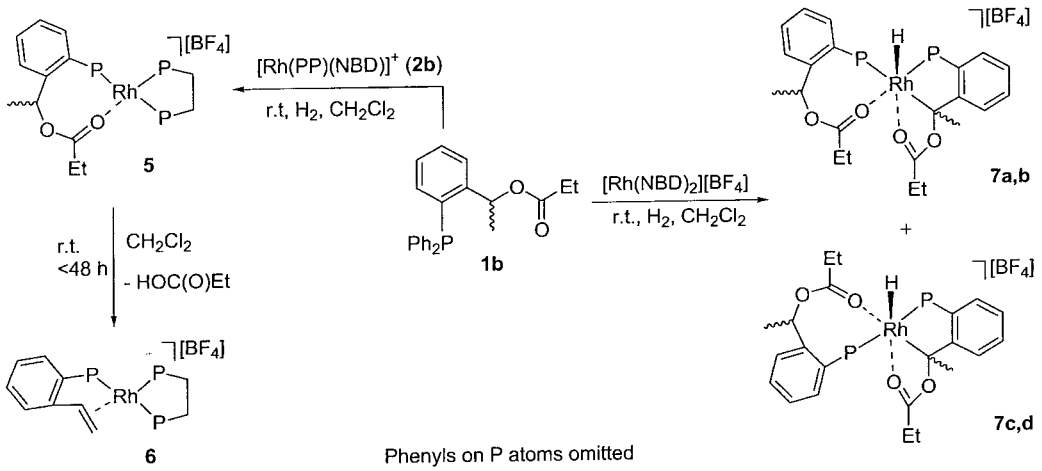

of this intermediate can take place either in an associative or in a dissociative fashion. Another alternative is that the agostic interaction seen in the crystal structure of **3b** is on the reaction path and that the activation takes place in the axial position. In this case it is less clear why the phosphine has to dissociate to promote reaction (except for giving a more electrophilic metal center, thus promoting the η^2-coordination), and we favor the first alternative.

Complexation of (±)-DPPES (1c) with Different Rhodium Precursors. With the possible objective of gaining insight into the important C−C bond activation process of an unstrained saturated carbon−carbon bond, the (±)-DPPES ligand (**1c**) (Scheme 1) and its complexation behavior were also investigated. Pioneering work by Milstein and co-workers have shown that C−C activation can be kinetically and thermodynamically competitive with C−H activation under appropriate conditions.[4j,k] Ligand **1c**, having only one benzylic C−H bond and being bulkier than **1a** due to steric hindrance imposed by the methyl group, may allow for a competition between C−H and C−C bond activation processes. We considered three different reaction pathways, namely (i) C−H bond activation of the benzylic carbon−hydrogen bond, forming a five-membered chelate, (ii) C−H bond activation of the methyl carbon−hydrogen bond, forming a six-membered chelate, and (iii) C−C bond activation of the benzylic carbon−methyl bond, forming a five-membered chelate.

Upon reaction of **1c** with [Rh(DPPE)(NBD)][BF_4] (**2b**) (Scheme 4) in the presence of molecular hydrogen, complex **5** was formed and spectroscopically characterized. The NMR spectra of **5** were very similar to those of **3b**, except for the signals arising from the tertiary benzylic group. The existence of the eight-membered chelate was further verified by an IR spectrum, displaying a stretching frequency for the carbonyl group at 1661 cm^{-1} (1729 cm^{-1} for free (±)-DPPES). However, the stability of complex **5** deviates substantially from that observed for **3b**; an NMR sample kept at room temperature for some hours showed that complex **5** underwent slow, clean thermolysis. After more than 48 h at room temperature a $^{31}P\{^1H\}$ NMR spectrum of the sample taken at 263 K still displayed three doublets of doublets of doublets, but now at completely different chemical shifts located at 63.9 ($^1J_{RhP}$ = 120.9 Hz, $^2J_{PP}$ = 316.8, 26.8 Hz), 53.9 ($^1J_{RhP}$ = 153.2 Hz, $^2J_{PP}$ = 31.1, 26.8 Hz), and 38.9 ppm ($^1J_{RhP}$ = 123.3 Hz, $^2J_{PP}$ = 316.8, 31.1 Hz). At this stage all peaks in the ^1H NMR spectrum related to the chelating sidearm in (±)-DPPES had been replaced by three broad signals of equal intensity located at 5.25, 4.18, and 3.65 ppm along with additional peaks at 2.35 and 1.18 ppm. This new compound was crystallized from a CH_2Cl_2/Et_2O solution of **5** (Scheme 4), and X-ray crystallography (vide infra) revealed the formation of [Rh(DPPSTY)(DPPE)][BF_4] (**6**; DPPSTY = 2-(diphenylphosphino)styrene). In an attempt to detect any kind of intermediates along the decomposition pathway by ^1H NMR, only the signals assigned to **5**, **6**, and propionic acid were observed.

Thus, the metal center mediates facile elimination of carboxylic acid from an ester, a process that normally requires very high temperatures (300−500 °C).[10] The mechanism for this unexpected transformation is not clear, but obviously there is yet another alternative in addition to the three we had anticipated: namely, C−O bond activation. A possible sequence to achieve this is oxidative addition of the C−O bond to give a Rh(III) benzyl species, which then can undergo β-hydride elimination followed by deprotonation to give the styrene complex and propionic acid. Given that this process is facile at room temperature, it probably does not involve opening of the strong chelate in DPPE. This can be understood in terms of the usual type mechanisms for oxidative addition. In the three-center addition displayed by nonpolar species, the coordination (in an η^2-fashion) of the C−H bond, which often dictates the reactivity, is promoted by coordinative unsaturation.[2,11] In the C−O addition, on the other hand, we have a fairly good leaving group and the S_N2 reaction usually displayed by polar species will be faster with a more electron-rich metal center.

Examples of transition-metal-mediated cleavage of carboxylic C−O ester bonds are fairly abundant, e.g., in the reaction of palladium(0) complexes with allyl and benzyl carboxylates,[12] but we have found no examples in the literature of room-temperature eliminations of

(10) Depuy, C. H.; King, R. W. *Chem. Rev.* **1960**, *60*, 431.
(11) McNamara, B. K.; Yeston, J. S.; Bergman, R. G.; Moore, C. B. *J. Am. Chem. Soc.* **1999**, *121*, 6437.
(12) (a) Yamamoto, A. *Adv. Organomet. Chem.* **1992**, *34*, 111. (b) Nagayama, K.; Shimizu, I.; Yamamoto, A. *Bull. Chem. Soc. Jpn.* **1999**, *72*, 799.

carboxylic acids to give olefins. Further studies are underway to explore the mechanism behind this unusual transformation.

The unexpected chemical behavior of the (±)-DPPES ligand calls for a different rhodium precursor than has been used up to now.[13] To favor concerted C−X (X = C, H) bond addition, we need a more labile rhodium complex, with or without ancillary ligands. Accordingly, a dichloromethane solution of $[Rh(NBD)_2][BF_4]$ was treated with 2 equiv of (±)-DPPES under an atmosphere of hydrogen at room temperature for 5 min to form complex **7** (Scheme 4). The ratio of cis/trans isomers varies slightly from batch to batch but is always approximately 3:2 in favor of the cis isomer. The $^{31}P\{^1H\}$ NMR spectrum of **7** at 253 K displays a total of eight doublets of doublets: at 58.5 and 19.7 ppm ($^2J_{PP}$ = 36.3 Hz) for **7a**, 58.2 and 15.6 ppm ($^2J_{PP}$ = 36.0 Hz) for **7b**, 43.4 and 27.4 ppm ($^2J_{PP}$ = 358.3 Hz) for **7c**, and 41.5 and 31.3 ppm ($^2J_{PP}$ = 371.1 Hz) for **7d**. In the ^1H NMR spectrum at 253 K two multiple hydride signals are displayed at −21.9 (**7c**,**d**) and −23.3 ppm (**7a**,**b**). Evidently, in this case the C−H activation process is the kinetically preferred one. It is undoubtedly the benzylic carbon that becomes metalated, as evidenced by the $^{31}P\{^1H\}$ NMR shifts for the cyclometalated (±)-DPPES ligands. Only five-membered chelate formation results in such a strong downfield shift, compared to the shift for the eight-membered P,O-chelating (±)-DPPES ligand.[14] Each set of cis−trans isomers consists of a 1:1 mixture of diastereomers. This is what one would expect with one stereogenic center on each of the ligands. In addition there is a possibility for two configurations along the Rh−C bond, where the vicinal hydride and methyl group can be either anti or gauche. This could potentially give even more stereoisomers, and obviously only one configuration is formed. In analogy with what was earlier exclusively observed in the crystal structures of PCO chelates of **1a**,**b** with Rh and Ir, respectively, the conformation is probably gauche.[6b,c]

The observed reaction with the (±)-DPPES ligand is, to the best of our knowledge, the first example of a phosphine derivative capable of cyclometalation via a tertiary carbon at room temperature. Previously, Shaw and co-workers have described a number of cyclometalated platinum group metal complexes derived from the sterically hindered $^tBu_2P(o\text{-}^iPrC_6H_4)$ and $^tBu_2PCH_2CH_2CHMeCH_2CH_2P^tBu_2$ ligands, all synthesized at elevated temperatures.[15] There can be several reasons for why (±)-DPPES follows the C−H oxidative addition pathway exclusively in complexes **7a**−**d**. Clearly, the P,O chelate is very fluxional, thus enabling a similar trans arrangement of the (other) P,O ligand just as proposed for **3a**,**b** in the formation **4a**,**b**, and this promotes concerted over S_N2 addition. Even though C−C bond activation has been shown to kinetically compete with C−H activation,[4j,k] all examples so far involve $C_{sp^2}-C_{sp^3}$ bonds and on the basis of the exclusive formation of **7** it seems reasonable to believe that the $M-C_{sp^3}$ bond is too weak to be formed at the expense of an M−H bond.

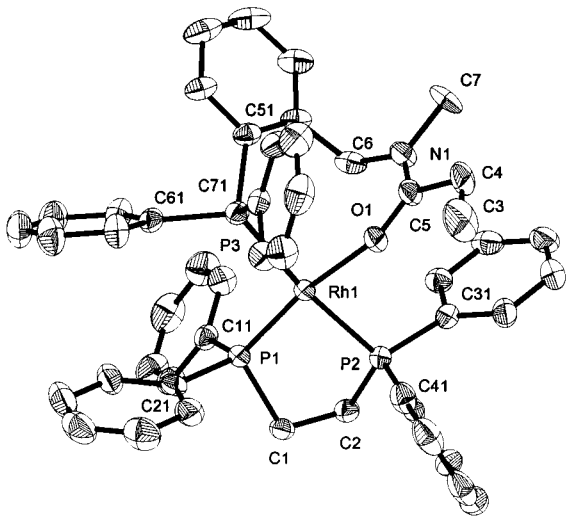

Figure 3. DIAMOND[17] plot of cation **3b**. For clarity, atomic numbering in the phenyl rings is only shown for the ipso carbons. Selected bond distances (Å) and angles (deg) with estimated standard deviations: Rh1−P1 = 2.180(1); Rh1−P2 = 2.254(1); Rh1−P3 = 2.310(1); Rh1−O1 = 2.120(3); P1−Rh1−P2 = 85.17(4); P1−Rh1−P3 = 101.68(4); P2−Rh1−P3 = 173.11(4); P1−Rh1−O1 = 170.74(8); P2−Rh1−O1 = 87.97(7); P3−Rh1−O1 = 85.29(7).

Crystal Structures. Yellow prismatic crystals of complex **3b** were obtained upon crystallization by layering Et_2O on top of a CH_2Cl_2 solution of **3b**. The structure consists of cationic rhodium complexes with tetrafluoroborate anions. The molecular structure of the cation is shown in Figure 3, including selected bond lengths and angles. The coordination geometry around rhodium is distorted square-planar with the three phosphorus atoms and the carbonyl oxygen in the corners of the square. Inter alia, the distortion results from ring strain in both chelate rings (P1−Rh1−P2 = 85.17(4)° and P3−Rh1−O1 = 85.29(7)°). The largest deviation from a least-squares plane through Rh1−P1−P2−P3−O1 is 0.082 Å, displayed by O1. The difference in Rh−P bond distances in the DPPE ligand manifests the different trans influences exerted by a phosphorus and an oxygen atom, respectively.[16] Interestingly, the Rh1−P3 bond length of 2.310(1) Å in the DPPAM ligand is almost identical with that observed in the cyclometalated rhodium(III) compound $[RhH(DPPAM)(PPh_3)_2][PF_6]$ ($Rh-P_{DPPAM}$ = 2.317(2) Å).[6c] Furthermore, the crystal structure reveals a bridging benzylic group (C6 positioned 3.090(6) Å away from the metal center). The positions of the hydrogen atoms on C6 were located in the difference Fourier map and successfully refined. Thus, H6B is located in an apical position 2.16(5) Å away from Rh, indicating a relatively weak agostic interaction.[18]

Slow vapor diffusion of Et_2O into a CH_2Cl_2 solution of **5** at room temperature resulted in formation of deep red crystals of complex **6**. The asymmetric unit of the structure consists of two independent cationic rhodium

(13) Using $[Rh(PPh_3)_2(NBD)][BF_4]$ as the precursor gave the same thermolysis reaction as the corresponding DPPE complex, although at a higher rate.

(14) (a) Garrou, P. E. *Chem. Rev.* **1981**, *81*, 229. (b) Lindner, E.; Fawzi, R.; Mayer, H. A.; Eichele, K.; Hiller, W. *Organometallics* **1992**, *11*, 1033.

(15) (a) Gill, D. F.; Shaw, B. L. *J. Chem. Soc., Chem. Commun.* **1972**, 65. (b) Crocker, C.; Errington, R. J.; Markham, R.; Moulton, C. J.; Odell, K. J.; Shaw, B. L. *J. Am. Chem. Soc.* **1980**, *102*, 4373.

(16) Appleton, T. G.; Clark, H. C.; Manzer, L. E. *Coord. Chem. Rev.* **1973**, *10*, 335.

(17) Brandenburg, K., DIAMOND, Program for Molecular Graphics; Crystal Impact, Bonn, Germany, 2000.

(18) Crabtree, R. H.; Holt, E. M.; Lavin, M.; Morehouse, S. M. *Inorg. Chem.* **1985**, *24*, 1986.

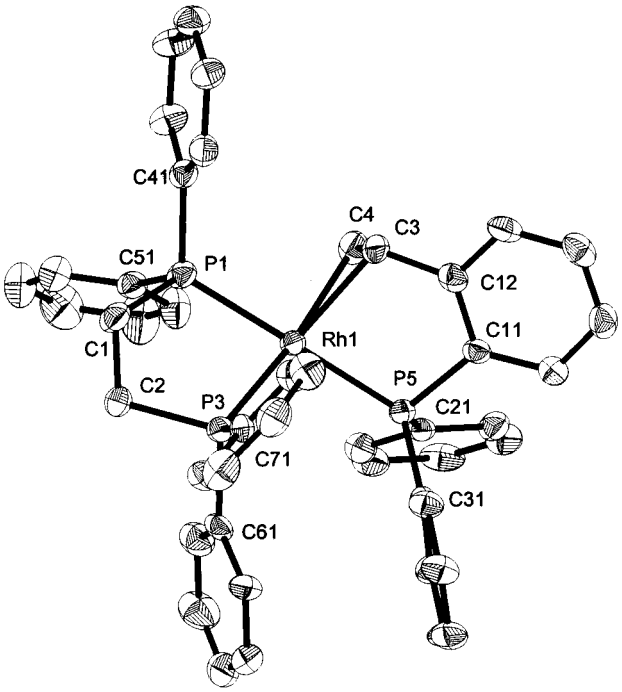

Figure 4. DIAMOND[17] plot of cation **6**. Only one of the asymmetric units is shown. For clarity, atomic numbering in the phenyl rings is only shown for the ipso carbons.

Table 1. Selected Bond Distances (Å) and Angles (deg) in 6

	Bond Lengths		
Rh1−C3	2.216(6)	Rh2−C7	2.201(6)
Rh1−C4	2.225(5)	Rh2−C8	2.221(6)
Rh1−P1	2.2904(18)	Rh2−P6	2.2968(19)
Rh1−P3	2.2831(19)	Rh2−P4	2.2911(19)
Rh1−P5	2.2958(18)	Rh2−P2	2.2928(19)
C3−C4	1.372(7)	C7−C8	1.408(7)
	Bond Angles		
C3−Rh1−P3	142.89(18)	C7−Rh2−P4	140.99(17)
C4−Rh1−P3	173.22(18)	C8−Rh2−P4	172.10(17)
C3−Rh1−P1	99.26(17)	C7−Rh2−P6	101.26(18)
C4−Rh1−P1	90.46(17)	C8−Rh2−P6	90.01(16)
P3−Rh1−P1	83.18(7)	P4−Rh2−P6	83.00(7)
C3−Rh1− P5	82.65(17)	C7−Rh2−P2	82.20(18)
C4−Rh1−P5	87.41(17)	C8−Rh2−P2	87.00(16)
P3−Rh1−P5	99.16(7)	P4−Rh2−P2	100.52(7)

complexes, each with a tetrafluoroborate anion and one molecule of CH_2Cl_2. The molecular structure of one of the independent rhodium cations is shown in Figure 4. Selected bond lengths and angles are given in Table 1.

The coordination geometry around the rhodium centers can be rationalized as distorted square planar, where the three phosphorus atoms and the β-carbon in the vinyl group occupy the corners. The mean deviation from these planes is 0.0726 and 0.1133 Å for Rh1 and Rh2, respectively. The α carbons are located 1.34 and 1.39 Å above these planes in the two asymmetric units, respectively. Despite this apparent asymmetry of the vinyl group, it is clearly an η^2 coordination with M−C distances being slightly (but not significantly in asymmetric unit 1) longer for the β-carbons and the C−C axis being approximately perpendicular to the coordination plane (cf. Figure 4). As expected, the vinylic bonds are longer than those in, for example, ethylene (1.339(5) Å).[19] The counteranions show large disorder in some of their atoms; no attempts were made to resolve this.

(19) Costain, C. C.; Stoicheff, B. P. *J. Chem. Phys.* **1959**, *30*, 777.

Experimental Section

General Procedures. All experiments with metal complexes and phosphine ligands were carried out under an atmosphere of nitrogen in a Braun glovebox equipped with an inert gas purifier or using standard Schlenk or high-vacuum techniques. All nondeuterated solvents were refluxed over sodium/benzophenone ketyl or CaH_2 and freshly distilled under a nitrogen atmosphere. Commercially available reagents were used as received. The complexes $[Rh(PP)(NBD)][BF_4]$[20] (PP = DPPB, DPPE), and $[Rh(NBD)_2][BF_4]$[21] and the phosphines 2-(diphenylphosphino)phenyl methyl ketone[22] and DPPAM[8] (**1a**) were prepared according to literature procedures.

NMR spectra were recorded either on a Varian Unity 300 MHz instrument (^{1}H, ^{31}P) or a Bruker ARX 500 MHz spectrometer (^{13}C) in $CDCl_3$ solvent unless otherwise stated. ^{1}H and $^{13}C\{^1H\}$ NMR chemical shifts are reported in ppm downfield from tetramethylsilane but were measured relative to the solvent residuals. ^{31}P NMR chemical shifts are reported in ppm downfield from an external 85% solution of phosphoric acid. NMR multiplicities are abbreviated as follows: s = singlet, d = doublet, t = triplet, q = quartet, m = multiplet, b = broad. Fast atom bombardment (FAB^+) mass spectroscopic data were obtained on a JEOL SX-102 spectrometer using 3-nitrobenzyl alcohol as matrix and CsI as calibrant. Infrared spectra were recorded on a Bio-Rad FTS 6000 FT-IR spectrometer. Mikro-Kemi AB, Uppsala, Sweden, performed elemental analyses.

Synthesis of (±)-DPPES (1c). A yellow suspension of 2-(diphenylphosphino)phenyl methyl ketone (3.02 g, 9.91 mmol) in 40 mL of THF/MeOH (1:1) was vigorously stirred. The mixture was cooled with an ice bath, and a pellet of $NaBH_4$ (1.02 g, 26.4 mmol) was added. After 1 h the ice bath was removed and the reaction mixture was stirred overnight. Addition of 40 mL of CH_2Cl_2 was followed by careful addition of degassed water (40 mL). The colorless organic phase was isolated, and the water phase was further extracted with CH_2Cl_2 (2 × 15 mL). The combined organic phases were dried over silica. Decanting and removal of the solvent resulted in a colorless, viscous oil. $^{31}P\{^1H\}$ NMR: δ −15.5 (s). ^{1}H NMR: δ 7.73−6.87 (m region, 14H, H_{Ar}), 5.62 (m, 1H, ArC*H*(CH_3)), 1.33 (d, $^3J_{HH}$ = 6.30 Hz, 3H, ArCH(C*H*$_3$)). The crude oil and pyridine (2.37 g, 30.0 mmol) were dissolved in 10 mL of THF. Propionyl chloride (0.897 mL, 10.3 mmol) was added carefully, and the suspension was stirred for 1.5 h. The white precipitate was removed by filtration through a plug of silica on a glass frit. Removal of the solvent resulted in a colorless, viscous oil. *n*-Pentane (100 mL) was added, and the cloudy solution was kept at −18 °C. The resulting white needles were isolated and dried under vacuum. Overall isolated yield: 2.73 g (76%). $^{31}P\{^1H\}$ NMR: δ −17.3 (s). ^{1}H NMR: δ 7.72−6.91 (m region, 14H, H_{Ar}), 6.64 (m, 1H, ArC*H*(CH_3)), 2.26−1.96 (m region, 2H, C*H*$_2$-CH_3), 1.37 (d, $^3J_{HH}$ = 6.3 Hz, 3H, ArCH(C*H*$_3$)), 1.04 (t, $^3J_{HH}$ = 7.2 Hz, 3H, CH_2C*H*$_3$). $^{13}C\{^1H\}$ NMR: δ 173.2 (s, *C*=O), 146.9−125.8 (m region, C_{Ar}), 70.0 (d, $^3J_{PC}$ = 28.1 Hz, Ar*C*H(CH_3)), 27.5 (s, *C*H$_2$CH$_3$), 21.9 (s, ArCH(*C*H$_3$)), 9.0 (s, CH$_2$*C*H$_3$). IR (KBr): 1729 cm^{-1} (s, C=O). Anal. Calcd for $C_{23}H_{23}O_2P$: C, 76.2; H, 6.4. Found: C, 76.0; H, 6.6.

Reaction of [Rh(DPPB)(NBD)][BF$_4$] (2a) with Phosphine 1a. Formation of [Rh(DPPAM)(DPPB)][BF$_4$] (3a). Dichloromethane (10 mL) was added to a Schlenk tube containing $[Rh(DPPB)(NBD)][BF_4]$ (118 mg, 0.166 mmol), DPPAM (**1a**; 60.6 mg, 0.167 mmol), and a magnetic stirring bar, and this resulted in an orange solution. A freeze−pump−thaw cycle replaced the argon atmosphere with molecular hydrogen. The closed Schlenk tube was allowed to reach room temperature and then stirred for 40 min, resulting in a yellow-tinted solution. Once again the atmosphere was replaced, this

(20) Fairlie, D. P.; Bosnich, B. *Organometallics* **1988**, *7*, 936.
(21) Uson, R.; Oro, L. A.; Garralda, M. A.; Claver, M. C.; Lahuerta, P. *Transition Met. Chem.* **1979**, *4*, 55.
(22) Schiemenz, G.; Kaack, H. *Liebigs Ann. Chem.* **1973**, 1494.

time from molecular hydrogen to argon, and the solution was allowed to stand for 5 min. Removal of the solvent under vacuum gave a yellow powder, which was washed with 1 × 10 mL of Et_2O and 2 × 10 mL of *n*-hexane. Finally, the air-stable compound **3a** was dried under vacuum. Yield: 148 mg (91%). $^{31}P\{^1H\}$ NMR (CD_2Cl_2): δ 48.9 (ddd, $^1J_{RhP}$ = 188.5 Hz, $^2J_{PP}$ = 51.1, 34.5 Hz, P_{DPPB}), 39.0 (ddd, $^1J_{RhP}$ = 145.1 Hz, $^2J_{PP}$ = 302.7, 51.1 Hz, P_{DPPB}), 30.3 (ddd, $^1J_{RhP}$ = 132.3 Hz, $^2J_{PP}$ = 302.7, 34.5 Hz, P_{DPPAM}). ^1H NMR (CD_2Cl_2): δ 8.98 (bd, $^2J_{HH}$ = 14.4 Hz, 1H, ArCH_2), 8.35−6.03 (m region, 34H, H_{Ar}), 3.81 (bd, $^2J_{HH}$ = 14.4 Hz, 1H, ArCH_2), 2.53 (s, 3H, NCH_3), 2.50−0.90 (m region, 10H, CH_2CH$_3$ and CH_2), −0.13 (t, $^3J_{HH}$ = 7.0 Hz, 3H, CH$_2$CH_3). $^{13}C\{^1H\}$ NMR (CD_2Cl_2): δ 175.6 (s, *C*═O), 139.6−129.3 (m region, C_{Ar}), 37.3 (s, NCH$_3$), 36.2 (m, *C*H$_2$), 30.2 (bs, *C*H$_2$), 29.9 (bs, *C*H$_2$), 29.5 (s, Ar*C*H$_2$), 26.0 (s, *C*H$_2$-CH$_3$), 25.1 (bs, *C*H$_2$), 9.4 (s, CH$_2$*C*H$_3$). IR (KBr): 1586 cm^{-1} (s, C═O). Anal. Calcd for $C_{51}H_{52}BF_4NOP_3Rh$: C, 62.6; H, 5.4. Found: C, 62.3; H, 5.5.

Reaction of [Rh(DPPE)(NBD)][BF$_4$] (2b) with Phosphine 1a. Formation of [Rh(DPPAM)(DPPE)][BF$_4$] (3b). Using a procedure identical with that for **3a** using [Rh(DPPE)(NBD)][BF_4] (49.9 mg, 73.4 μmol) and DPPAM (**1a**; 26.7 mg, 73.9 μmol) gave complex **3b** as an air-stable yellow powder. Yield: 57.9 mg (83%). $^{31}P\{^1H\}$ NMR: δ 79.4 (ddd, $^1J_{RhP}$ = 195.9 Hz, $^2J_{PP}$ = 37.3, 30.9 Hz, P_{DPPE}), 66.3 (ddd, $^1J_{RhP}$ = 144.7 Hz, $^2J_{PP}$ = 308.9, 37.3 Hz, P_{DPPE}), 29.4 (ddd, $^1J_{RhP}$ = 127.3 Hz, $^2J_{PP}$ = 308.9, 30.9 Hz, P_{DPPAM}). ^1H NMR: δ 8.48 (bd, $^2J_{HH}$ = 13.6 Hz, 1H, ArCH_2), 8.17−6.34 (m region, 34H, H_{Ar}), 4.07 (bd, $^2J_{HH}$ = 13.6 Hz, 1H, ArCH_2), 2.75 (s, 3H, NCH_3), 2.51−0.86 (m region, 6H, CH_2CH$_3$ and CH_2), 0.25 (t, $^3J_{HH}$ = 7.3 Hz, 3H, CH$_2$CH_3). $^{13}C\{^1H\}$ NMR: δ 175.6 (s, *C*═O), 137.2−128.2 (m region, C_{Ar}), 52.8 (m, *C*H$_2$), 40.8 (m, *C*H$_2$), 36.6 (s, N*C*H$_3$), 35.7 (s, Ar*C*H$_2$), 28.0 (s, *C*H$_2$CH$_3$), 8.8 (s, CH$_2$*C*H$_3$) (assignments of ^1H and $^{13}C\{^1H\}$ NMR signals were confirmed by an HMQC NMR experiment). IR (KBr): 1601 cm^{-1} (s, C═O). Anal. Calcd for $C_{49}H_{48}BF_4NOP_3Rh$: C, 62.0; H, 5.1. Found: C, 61.8; H, 5.1.

Conversion of Complex 3a to [RhH(DPPAM)(DPPB)][BF$_4$] (4a). A Schlenk tube was charged with [Rh(DPPAM)(DPPB)][BF_4] (**3a**; 72.2 mg, 73.9 μmol), a magnetic stirring bar, and 10 mL of THF. The vessel was closed, and the stirred solution was heated at 100 °C for 90 min, resulting in a color change from bright to light yellow. Evaporation of the solvent under vacuum gave **4a** as an off-white powder in a quantitative yield. $^{31}P\{^1H\}$ NMR (CD_2Cl_2): δ 56.1 (ddd, $^1J_{RhP}$ = 109.5 Hz, $^2J_{PP}$ = 372.6, 22.5 Hz, P_{DPPAM}), 40.0 (ddd, $^1J_{RhP}$ = 110.7 Hz, $^2J_{PP}$ = 372.6, 28.8 Hz, P_{DPPB}), 17.7 (ddd, $^1J_{RhP}$ = 83.7 Hz, $^2J_{PP}$ = 28.8, 22.5 Hz, P_{DPPB}). ^1H NMR (CD_2Cl_2): δ 7.82−6.47 (m region, 34H, H_{Ar}), 3.81 (bd, $^2J_{RhH}$ = 17.7 Hz, 1H, ArC*H*Rh), 2.52−0.70 (m region, 10H, CH_2CH$_3$ and CH_2), 2.09 (s, 3H, NCH_3), 0.54 (t, $^3J_{HH}$ = 7.4 Hz, 3H, CH$_2$CH_3), −17.2 (m, 1H, Rh*H*). $^{13}C\{^1H\}$ NMR (CD_2Cl_2): δ 179.4 (s, *C*═O), 135.9−128.5 (m region, C_{Ar}), 72.6 (m, Ar*C*HRh), 35.1 (d, $^3J_{RhC}$ = 4.2 Hz, N*C*H$_3$), 31.3 (d, $^1J_{PC}$ = 21.0 Hz, *C*H$_2$), 28.5 (m, *C*H$_2$), 26.9 (s, *C*H$_2$CH$_3$), 25.3 (d, $^2J_{PC}$ = 4.8 Hz, *C*H$_2$), 21.7 (bs, *C*H$_2$), 8.4 (s, CH$_2$*C*H$_3$). IR (KBr): 1571 cm^{-1} (s, C═O). MS (FAB$^+$): *m*/*z* 890 [$C_{51}H_{52}NOP_3Rh^+$]. Anal. Calcd for $C_{51}H_{52}BF_4NOP_3Rh$: C, 62.6; H, 5.4. Found: C, 62.3; H, 5.5.

Conversion of Complex 3b to [RhH(DPPAM)(DPPE)][BF$_4$] (4b). Using a procedure identical with that for **4a** using [Rh(DPPAM)(DPPE)][BF_4] (**3b**; 50.2 mg, 52.9 μmol) gave complex **4b** as an off-white powder in quantitative yield. $^{31}P\{^1H\}$ NMR (CD_2Cl_2): δ 69.4 (ddd, $^1J_{RhP}$ = 108.4 Hz, $^2J_{PP}$ = 370.8, 15.6 Hz, P_{DPPE}), 61.9 (ddd, $^1J_{RhP}$ = 108.7 Hz, $^2J_{PP}$ = 370.8, 20.3 Hz, P_{DPPAM}), 51.7 (ddd, $^1J_{RhP}$ = 83.2 Hz, $^2J_{PP}$ = 20.3, 15.6 Hz, P_{DPPE}). ^1H NMR (CD_2Cl_2): δ 7.97−6.78 (m region, 34H, H_{Ar}), 4.94 (m, 1H, ArC*H*Rh), 2.92−2.12 (m region, 4H, CH_2), 2.25 (s, 3H, NCH_3), 1.10−0.96 (m region, 2H, CH_2CH$_3$), 0.36 (t, $^3J_{HH}$ = 7.2 Hz, 3H, CH$_2$CH_3), −17.4 (m, 1H, Rh*H*). $^{13}C\{^1H\}$ NMR (CD_2Cl_2): δ 179.3 (s, *C*═O), 135.6−126.1 (m region, C_{Ar}), 70.9 (m, Ar*C*HRh), 46.4 (m, *C*H$_2$), 36.2 (m, *C*H$_2$), 34.8 (d, $^3J_{RhC}$ = 7.6 Hz, NCH$_3$), 28.7 (s, *C*H$_2$CH$_3$), 7.6 (s, CH$_2$*C*H$_3$). IR (KBr): 1572 cm^{-1} (s, C═O). MS (FAB$^+$): *m*/*z* 862 [$C_{49}H_{48}NOP_3Rh^+$]. Anal. Calcd for $C_{49}H_{48}BF_4NOP_3Rh$: C, 62.0; H, 5.1. Found: C, 61.7; H, 5.1.

Reaction of [Rh(DPPE)(NBD)][BF$_4$] (2b) with Phosphine 1c. Formation of [Rh((±)-DPPES)(DPPE)][BF$_4$] (5). Dichloromethane (10 mL) was added to a Schlenk tube containing [Rh(DPPE)(NBD)][BF_4] (**2b**; 63.8 mg, 93.8 μmol), (±)-DPPES (**1c**; 34.1 mg, 94.1 μmol), and a magnetic stirring bar, and this resulted in an orange solution. A freeze−pump−thaw cycle replaced the argon atmosphere with molecular hydrogen. The closed Schlenk tube was allowed to reach room temperature, and its contents were then stirred for 5 min, resulting in a light yellow solution. Once again the atmosphere was replaced, this time from molecular hydrogen to argon, and the solution was allowed to stand for 2 min. Concentration of the solution to ca. 1 mL, followed by addition of 10 mL of Et_2O/*n*-hexane (1:1), gave complex **5** as a light yellow precipitate. The powder was isolated by filtration and dried under vacuum. The complex was too unstable for microanalysis. Yield: 74.0 mg (83%). $^{31}P\{^1H\}$ NMR (CD_2Cl_2): δ 78.2 (ddd, $^1J_{RhP}$ = 205.3 Hz, $^2J_{PP}$ = 35.7, 31.9 Hz, P_{DPPE}), 65.8 (ddd, $^1J_{RhP}$ = 142.0 Hz, $^2J_{PP}$ = 298.1, 35.7 Hz, P_{DPPE}), 25.9 (ddd, $^1J_{RhP}$ = 127 Hz, $^2J_{PP}$ = 298.1, 31.9 Hz, P_{DPPES}). ^1H NMR (CD_2Cl_2): δ 9.05 (m, 1H, H_{Ar}), 8.12−6.62 (m region, 33H, H_{Ar}), 2.51−1.26 (m region, 5H, CH_2 and ArC*H*(CH$_3$)), 1.70 (d, $^3J_{HH}$ = 4.9 Hz, 3H, ArCH(CH_3)), 1.19−0.92 (m region, 2H, CH_2CH$_3$), 0.41 (t, 3H, $^3J_{HH}$ = 7.4 Hz, CH$_2$CH_3). IR (KBr): 1661 cm^{-1} (s, C═O). MS (FAB$^+$): *m*/*z* 863 [$C_{49}H_{47}O_2P_3Rh^+$].

Conversion of Complex 5 to [Rh(DPPSTY)(DPPE)][BF$_4$] (6). A tube containing [Rh((±)-DPPES)(DPPE)][BF_4] (**5**; 50.2 mg, 52.8 μmol), dissolved in 3 mL of CH_2Cl_2, was placed inside a Schlenk vessel containing Et_2O. After 7 days deep red, air-stable crystals of **6** were harvested from the inner tube. Yield: 33.3 mg (72%). $^{31}P\{^1H\}$ NMR (263 K): δ 63.9 (ddd, $^1J_{RhP}$ = 120.9 Hz, $^2J_{PP}$ = 316.8, 26.8 Hz, P_{DPPE}), 53.9 (ddd, $^1J_{RhP}$ = 153.2 Hz, $^2J_{PP}$ = 31.1, 26.8 Hz, P_{DPPE}), 38.9 (ddd, $^1J_{RhP}$ = 123.3 Hz, $^2J_{PP}$ = 316.8, 31.1 Hz, P_{DPPSTY}). ^1H NMR (263 K): δ 7.72−6.59 (m region, 34H, H_{Ar}), 5.25 (m, 1H, ArCHCH_2), 4.18 (m, 1H, ArC*H*CH$_2$), 3.65 (m, 1H, ArCHCH_2), 2.58−2.02 (m region, 4H, CH_2). Anal. Calcd for $C_{46}H_{41}BF_4P_3Rh\cdot{}^1/_2CH_2Cl_2$: C, 60.8; H, 4.6. Found: C, 60.6; H, 4.8.

Reaction of [Rh(NBD)$_2$][BF$_4$] with Phosphine 1c. Formation of [RhH((±)-DPPES)$_2$][BF$_4$] (7a−d). Using a procedure identical with that described for the formation of **5** but using [Rh(NBD)$_2$][BF_4] (28.3 mg, 75.6 μmol) and (±)-DPPES (**1c**; 55.3 mg, 0.152 mmol) gave complexes **7a**−**d** as yellow powders. Yield: 69.1 mg (81%). $^{31}P\{^1H\}$ NMR (253 K): δ 58.5 (dd, $^1J_{RhP}$ = 169.2 Hz, $^2J_{PP}$ = 36.3 Hz, P_{cis}, **7a**), 58.2 (dd, $^1J_{RhP}$ = 185.1 Hz, $^2J_{PP}$ = 36.0 Hz, P_{cis}, **7b**), 43.4 (dd, $^1J_{RhP}$ = 126.2 Hz, $^2J_{PP}$ = 358.3 Hz, P_{trans}, **7c**), 41.5 (dd, $^1J_{RhP}$ = 120.4 Hz, $^2J_{PP}$ = 371.1 Hz, P_{trans}, **7d**), 31.3 (dd, $^1J_{RhP}$ = 120.2 Hz, $^2J_{PP}$ = 371.1 Hz, P_{trans}, **7d**), 27.4 (dd, $^1J_{RhP}$ = 115.5 Hz, $^2J_{PP}$ = 358.3 Hz, P_{trans}, **7c**), 19.7 (dd, $^1J_{RhP}$ = 152.0 Hz, $^2J_{PP}$ = 36.3 Hz, P_{cis}, **7a**), 15.6 (dd, $^1J_{RhP}$ = 154.4 Hz, $^2J_{PP}$ = 36.0 Hz, P_{cis}, **7b**). ^1H NMR (253 K): δ −21.9 (m, Rh*H*, **7c**,**d**), −23.3 (m, Rh*H*, **7a**,**b**) (ratio 2:3) (assignments in the normal region impossible due to severe overlapping). IR (KBr): 1683 cm^{-1} (bs, C═O). Anal. Calcd for $C_{46}H_{46}BF_4O_4P_2Rh$: C, 60.4; H, 5.1. Found: C, 60.0; H, 5.2.

Structure Determinations. Crystal data and details about data collection are given in Table 2. The intensity data sets for both **3b** and **6** were collected at 293 K with a Bruker SMART CCD system using ω-scans and a rotating anode with Mo Kα radiation (λ = 0.710 73 Å).[23] The intensity was corrected for Lorentz, polarization, and absorption effects using SADABS.[24] In both structures the first 50 frames were

(23) BrukerAXS, SMART, Area Detector Control Software; Bruker Analytical X-ray Systems, Madison, WI, 1995.
(24) Sheldrick, G. M. SADABS, Program for Absorption Correction; University of Göttingen, Göttingen, Germany, 1996.

Table 2. Crystal Data for 3b and 6

	3b	6
formula	$C_{49}H_{48}BF_4NOP_3Rh$	$C_{46}H_{41}BF_4P_3Rh\cdot{}^1/_2CH_2Cl_2$
fw	949.51	918.88
space group	$P\bar{1}$	$P\bar{1}$
a/Å	11.4318(6)	4.804(3)
b/Å	13.0682(6)	14.977(3)
c/Å	15.9971(8)	20.943(4)
α/deg	85.4390(10)	75.61(3)
β/deg	84.3880(10)	87.31(3)
γ/deg	71.0460(10)	71.07(3)
V/Å^3	2246.55(19)	4251.4(15)
Z	2	4
D_{calcd}/g cm^{-3}	1.404	1.436
μ/mm^{-1}	0.541	0.628
θ range/deg	1.28−31.82	1.00−32.11
no. of rflns collected	23 520	44 146
no. of unique rflns	13 576	26 150
R^a	0.0550	0.0622
$R_w{}^b$	0.1070	0.1213
S^c	0.892	0.763
R_{int}	0.0613	0.1161

[a] $R = \sum(|F_o| - |F_c|)/\sum|F_o|$, [b] $R_w = [\sum w(|F_o| - |F_c|)^2/\sum|F_o|^2]^{1/2}$, [c] $S = [\sum w(|F_o| - |F_c|)^2/(m - n)]^{1/2}$

collected again at the end to check for decay and no decay was observed. All reflections were integrated using SAINT.[25] Both structures were solved by direct methods and refined by full-matrix least-squares calculations on F^2 using SHELXTL 5.1.[26] Non-H atoms were refined with anisotropic displacement parameters. Hydrogen atoms (except on methyl groups and on C6 in **3b**) were constrained to parent sites, using a riding model.

Kinetics Measurements. A J. Young NMR tube was charged with ca. 10 mg of complex **3b**, and 0.75 mL of 1,1,2,2-tetrachloroethane-d_2 was added. The conversion of **3b** was monitored by ^{1}H NMR spectroscopy at four different temperatures ranging from 332.7 to 362.7 K until at least 90% conversion. Temperatures were measured using ethylene glycol. No deuterium incorporation was observed during the reaction or in the final product upon standing.

Acknowledgment. We thank Prof. Åke Oskarsson for valuable discussions of the X-ray diffraction work. We are also grateful to Dr. Torsten Malmström, AstraZeneca, for running an HMQC experiment. We thank one reviewer for pointing out the possibility of different configurations with respect to the Rh−C bond in **7**. Financial support from the Swedish Natural Science Research Council and the Swedish Foundation for Strategic Research is gratefully acknowledged.

Supporting Information Available: Complete crystallographic data in the CIF format. This material is available free of charge via the Internet at http://pubs.acs.org. Data for complexes **3b** (CCDC 169397) and **6** (CCDC 169398) have also been deposited with the Cambridge Crystallographic Data Centre. Tables of structure factors are available from the authors upon request.

OM010543X

(25) BrukerAXS, SAINT, Integration Software; Bruker Analytical X-ray Systems, Madison, WI, 1995.

(26) Sheldrick, G. M. SHELXTL5.1, Program for Structure Solution and Least Squares Refinement; University of Göttingen, Göttingen, Germany, 1998.